Nanoscale

Accepted Manuscript

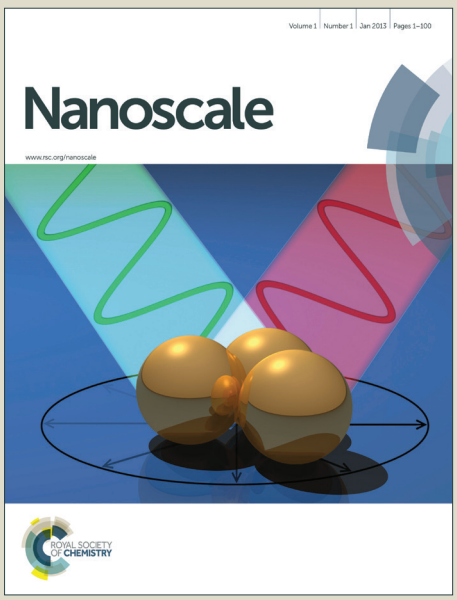

ROYAL SOCIETY OF CHEMISTRY

www.rsc.org/nanoscale

Theranostic Etoposide Phosphate/Indium Nanoparticles for Cancer Therapy and Imaging

Ramishetti Srinivas[1†], Andrew Satterlee[2†], Yuhua Wang[1], Yuan Zhang[1], Yongjun Wang[1] and Leaf Huang[1, 2]*

[1]Division of Molecular Pharmaceutics and Center for Nanotechnology in Drug Delivery, Eshelman School of Pharmacy, University of North Carolina at Chapel Hill, Chapel Hill, NC 27599, USA.
[2]UNC and NCSU Joint Department of Biomedical Engineering, Chapel Hill, NC 27599

[†]Authors contributed equally

* Corresponding address: leafh@unc.edu

Graphical Abstract:

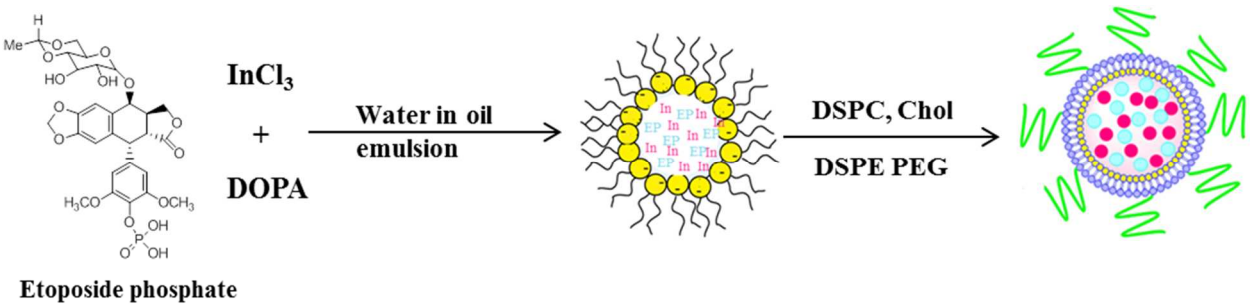

Theranostic Etoposide Phosphate/Indium Nanoparticles for Cancer Therapy and Imaging

Ramishetti Srinivas[1†], Andrew Satterlee[2†], Yuhua Wang[1], Yuan Zhang[1], Yongjun Wang[1] and Leaf Huang[1, 2]*

[†]Authors contributed equally
[1]Division of Molecular Pharmaceutics and Center for Nanotechnology in Drug Delivery, Eshelman School of Pharmacy, University of North Carolina at Chapel Hill, Chapel Hill, NC 27599, USA.
[2]UNC and NCSU Joint Department of Biomedical Engineering, Chapel Hill, NC 27599

* Corresponding address: leafh@unc.edu

Abstract:

Etoposide phosphate (EP), a water-soluble anticancer prodrug, is widely used for treatment of many cancers. After administration it is rapidly converted to etoposide, its parent compound, which exhibits anticancer activity. Difficulty in parenteral administration necessitates the development of a suitable nanoparticle delivery system for EP. Here we have used indium both as a carrier to deliver etoposide phosphate to tumor cells and as a SPECT imaging agent through incorporation of ^{111}In. Etoposide phosphate was successfully encapsulated together with indium in nanoparticles, and exhibited dose dependent cytotoxicity and induction of apoptosis in cultured H460 cancer cells via G2/M cell cycle arrest. In a mouse xenograft lung cancer model, etoposide phosphate/indium nanoparticles induce tumor cell apoptosis, leading to significant enhancement of tumor growth inhibition compared to the free drug.

Key words: Indium nanoparticles, Etoposide phosphate, Cell cycle arrest, Lung cancer therapy

Introduction:

Etoposide, an analog of the anti-cancer agent podophilotoxin, is clinically used for the treatment of several cancers including lung cancer and testicular cancer.[1] The mechanism of its anti-cancer activity involves inhibition of topoisomerase II, an enzyme responsible for DNA strand ligation during cell division. Cancer cells rely on this enzyme to a greater extent than healthy cells because of their rapid growth.[2] Etoposide forms a complex with DNA and topoisomerase II and prevents re-ligation of the DNA strand, resulting in strand breakage and subsequent apoptosis. Due to the limited solubility of etoposide, a water soluble prodrug named Etoposide phosphate (EP) was synthesized.[3] EP is readily metabolized *in vivo* to its parent molecule, Etoposide, for anticancer activity.[3-5] Although administration of EP resolved the solubility issue, parenteral administration of EP frequently causes leukopenia and neutropenia in patients. These adverse effects underscore the need for a nanoparticle delivery system to carry EP to the appropriate cells after systemic administration.

Over the past few decades, there have been major diagnostic and therapeutic advances in cancer nano medicine.[6] Nanoparticles can extravasate through leaky tumor vasculature and preferentially accumulate in tumor tissue due to the enhanced permeability and retention (EPR) effect.[7, 8] A number of nanoparticle systems based on liposomes, polymers, inorganic materials, etc. have been developed for delivery of anticancer drugs and imaging agents to tumors. The subject has been recently reviewed.[9]

Previous reports have demonstrated *in vitro* delivery of etoposide using different nanoparticle formulations, including single-walled nanotubes modified with epidermal growth factor,[10] strontium carbonate,[11] lipid nano capsules (LNC)[12] and other polymer-based nanoparticles.[13-16] In a recent study, intra-tumoral injection of etoposide encapsulated in poly

(ethylene glycol)-co-poly (sebacic acid) (PEG-PSA) polymeric nanoparticles exhibited significant antitumor activity compared to control in an NCI-H82 xenograft mouse model,[17] but this intra-tumoral route of administration has not been established as an alternative in routine clinical practice.

Transition metal cations like indium readily precipitate phosphorylated compounds at neutral pH, and we found that EP could be readily precipitated by $InCl_3$. We took advantage of the In-EP complex and used this nanoprecipitate to deliver EP to tumor cells. This manuscript describes the first time an indium-based nanoparticle drug delivery system has been reported for EP. Because a radioactive isotope of indium, ^{111}In, is also an excellent contrast agent for diagnostic imaging by single photon emission computed tomography (SPECT), this complex was also used as a theranostic agent.[18-21]

In the present manuscript, we propose the synthesis of a nano-sized, lipid-stabilized indium-EP complex using a reverse micro emulsion system. The surface of the nanoparticles was highly PEGylated to increase dispersion during fabrication and stability in circulation and reduce nonspecific uptake by the mononuclear phagocyte system (MPS). Here, we characterize the *in vitro* and *in vivo* performance of these nanoparticles.

Experimental

Materials:

Etoposide phosphate was purchased from Carbosynth (UK), 2-Dioleoyl-3-trimethylammonium-propanechloride salt (DOTAP), dioleoylphosphatydic acid (DOPA), and 1,2-distearoryl-snglycero-3-phosphoethanolamine-N-[methoxy(polyethyleneglycol-2000) ammonium salt

(DSPE-PEG2000) were purchased from Avanti Polar Lipids, Inc. (Alabaster, AL). All other chemicals were obtained from Sigma-Aldrich (St. Louis, MO) unless otherwise mentioned.

Cell culture:

H460 human NSCLC cells, obtained from American Type Culture Collection (ATCC), were cultured in an RPMI-1640 medium (Invitrogen, Carlsbad, CA) supplemented with 10% fetal bovine serum, 100 U/mL penicillin, and 100 mg/mL streptomycin (Invitrogen). Cells were cultivated in a humidified incubator at 37°C and 5% CO_2.

Experimental animals:

Female nude mice and CD-1 mice of 6-8 weeks age were purchased from National Cancer Institute (Bethesda, MD) and bred in the Division of Laboratory Animal Medicine (DLAM) at University of North Carolina at Chapel Hill. To establish the xenograft models, $5x10^6$ cells in 50 μL of PBS were injected subcutaneously into the right flank of the mice. All work performed on animals was approved by the Institutional Animal Care and Use Committee at the University of North Carolina at Chapel Hill.

Preparation of Etoposide phosphate loaded Indium nanoparticles (IEP-PEG):

The IEP core particles were prepared as reported previously with some modifications.[22] Two hundred and fifty μL of 20 mM etoposide phosphate solution was added to 20 mL oil phase containing a cyclohexane/IgepalCO-520/triton-100/Hexanol solution (71.25/22.5/3.75/2.5, v/v) with continuous stirring. Another micro emulsion was prepared by adding 250uL of 100 mM Indium chloride in water to 20ml of the described oil phase. 300 μL of DOPA (25mg/mL) solution was added to the oil phase containing EP. After five minutes, two separate micro-emulsions were mixed and stirred continuously for 20 min before the addition of 40 mL of absolute ethanol. The resultant solution was centrifuged at 10000 x g for 20 min to pellet the IEP

core, and the supernatant was removed. This washing procedure was repeated twice to remove any excess surfactant. The remaining precipitate was dissolved in chloroform and centrifuged once again at 10000 x g for 5 min to remove any non DOPA-coated precipitate. The DOPA-coated core particles dissolved in chloroform could then be stored at -20°C for at least 1 month before use. The final particles were made by adding 20mM DOPC, Chol and DSPE-PEG (1:1:0.5 mole ratios) dissolved in chloroform to the IEP cores. The ratio of total outer leaflet lipid volume to total oil phase volume is 0.044:1. The solvent was then removed under reduced pressure to form a dry lipid film. The final particles were prepared by hydration with 80^{o}C water and sonication.

Characterization of IEP-PEG nanoparticles:

Transmission electron microscope (TEM) images of IEP core particles were acquired by JEOL 100CX II TEM (Tokyo, Japan). The Energy dispersive X-ray spectroscopy (EDS) results were obtained by JEOL 2010F FaSTEM, 200kV accelerating voltage connected to Oxford X-mas system. A 300 mesh carbon coated copper grid (Ted Pella, Inc., Redding, CA) was used to prepare samples for TEM and EDS. The particle size and zeta potential of final, lipid coated IEP-PEG nanoparticles were determined by dynamic light scattering (DLS) using a Malvern ZetaSizer Nano series (Westborough, MA). Encapsulation efficiency (EE) of EP was measured by a UV/Vis spectrophotometer (Beckman Coulter Inc., DU 800). The mass spectrum was obtained using LCMS (Shimadzu).

***In vitro* cellular uptake of IEP-PEG:**

Cellular uptake of IEP-PEG nanoparticles by H460 cancer cells was observed by using dual labeled nanoparticles. The particle cores were labeled with NBD-DOPA and lipid bilayer was

labeled with DiI. The labeled particles were incubated with cells for 4 h, washed twice with PBS, and fixed with 4% paraformaldehyde. Nuclei were stained with DAPI (Vector laboratories, CA). Fluorescent pictures were taken using an Olympus FV1000 MPE SIM Laser Scanning Confocal Microscope (Olympus).

In vitro release of IEP-PEG:

The *in vitro* release of EP from IEP-PEG was measured in triplicate at two different pH levels of PBS: pH 7.4 and pH 5. Approximately 150 nmol of EP in IEP-PEG was diluted to 200ul in water and was added to 300 µl of PBS in the upper chamber of a Slide-A-Lyzer dialysis tube, MW cutoff 3.5kDa. The lower chamber was filled with 14 ml of PBS to act as a sink condition, and the entire apparatus was shaken at 120 RPM and 37^{o}C. At t = 0.5, 1, 2, 4, 8, 16, 24, and 48 h, the lower chamber was emptied into another vial and replaced with fresh PBS. At the end of the study, all samples were lyophilized and re suspended in 400 µl of water. The UV absorption of each sample was then read and compared against an EP standard curve (max Abs = 288 nm) to reconstruct the release profile.

***In vivo* pharmacokinetics and bio-distribution:**

^{111}IEP-PEG nanoparticles were fabricated by mixing a trace amount of ^{111}In ($^{111}InCl_3$, PerkinElmer, Inc.) with the EP aqueous phase just before its addition to the microemulsion. *In vivo* pharmacokinetics of ^{111}IEP-PEG were conducted by injecting ^{111}IEP-PEG i.v. into the mouse tail vein, extracting a small volume of blood at several time points, and reading the signal from ^{111}In using gamma scintillation. Bio-distribution of ^{111}IEP-PEG nanoparticles was also measured in H460 tumor-bearing nude mice after i.v. injection of ^{111}IEP-PEG. 2 h or 24 h after injection, mice were sacrificed, their organs were dissected, and the ^{111}In signal in each organ

was read. In addition, one mouse was given a dose of ~1.1 mCi of ^{111}IEP-PEG and the bio-distribution in the live mouse was measured at t= 2h using SPECT imaging.

***In vitro* cell viability assay (MTT):**

In vitro cell viability of IEP-PEG nanoparticles was determined by using the 3-[4, 5-dimethylthiazol-2-yl]-2, 5-diphenyltetrazolium bromide (MTT) assay. H460 cells were seeded at a density of $1x10^4$ per well in 96-well plates 24 h prior to treatment. The cells were incubated with different concentrations of IEP-PEG, free $InCl_3$, free outer liposome and free etoposide phosphate in serum free Opti-MEM (Gibco) media, after four hours the medium was replaced with complete medium (RPMI1640 + 10% FBS), The concentrations of $InCl_3$ and free liposomes were maintained in equal amounts used for IEP-PEG. After 36 h, the medium was replaced with fresh medium containing 5% MTT (Biosynth Inc.) solution and incubated at 37 °C for another 4h. The resulting formazan crystals were solubilized by adding 100 µL DMSO/Methanol (50:50) solution to each well. The absorbance at 570 nm was measured with a micro plate reader. Cell viability was calculated as the (absorbance of treated cells)/(absorbance of untreated cells)*100%.

Caspase activation assay:

H460 cells ($2x10^5$) were treated with nanoparticles containing 25 µM EP, or with relevant controls for 4h in serum free Opti-MEM, after which the medium was replaced with complete medium containing RPMI 1640 with 10% FBS. After 36 h, the cells were lysed with a radio-immunoprecipitation assay (RIPA) buffer that was supplemented with a protease inhibitor cocktail (Promega, Madison, WI). The protein lysates were collected by centrifugation at 14,000 rpm for 10 min at 4°C. Protein concentrations were determined using the BCA assay kit (Pierce Biotechnology) following the manufacturer's recommendations. Thirty micrograms protein of

each sample was used to detect caspase-3/7 activity of the cell lysates by using an *in vitro* assay kit according to the manufacturer's instructions (Promega).

Western blot analysis for PARP:

Forty micrograms of protein per lane, prepared as in the above section, was resolved by 4-12% SDS-PAGE Electrophoresis (Invitrogen) before being transferred to polyvinylidenedifluoride (PVDF) membranes (Bio-Rad). The membranes were blocked for 1 h with 5% skim milk at room temperature and then incubated with a mouse monoclonal poly (ADPribose) polymerase-1 (PARP-1) antibody (1:500 dilution; Santa Cruz biotechnology, Inc.) and with a β-actin antibody (1:4,000 dilution; Santa Cruz biotechnology, Inc.) overnight at 4°C. β-actin was probed as the loading control. The membranes were washed 3 times and then incubated with a secondary antibody (1:4,000 dilutions; Santa Cruz biotechnology, Inc.) at room temperature for 1 h. Goat anti-mouse secondary antibody was used for PARP and β-actin primary antibody. The membranes were washed 4 times and developed by an enhanced chemiluminescence system according to the manufacturer's instructions (Thermo scientific).

Cell cycle analysis:

$2x10^5$ H460 cells were seeded in 6-well plates 24h prior to treatment with nanoparticles containing 25 μM EP, or with relevant controls in serum-free Opti-MEM for four h, after which the media was replaced with RPMI1640 + 10% FBS. The cells were then incubated for 24 h at 37 °C in a humidified CO_2 incubator. The cells were trypsinized and washed with PBS, followed by fixation in pre-cooled 70% ethanol at -20 °C for >1 h. Fixed cells were washed with PBS staining buffer (BD Pharmingen, San Diego, CA) and incubated with RNAase (final concentration 75 mg/mL) at 37 °C for 30 min, followed by incubation with 10 mg propidium iodide (PI) at room temperature for 30 min. Finally, cells were washed and suspended in PBS,

and analyzed with a FACS Canto flow cytometer (BD Biosciences) to measure the PI intensity, which correlates with the DNA content in the cell cycle. A total of 20,000 events were acquired for each sample and data were analyzed with FACS Diva software (BD Biosciences).

Tumor growth inhibition studies:

A tumor growth inhibition study was completed on H460 subcutaneous xenograft mouse models. Mice were inoculated with $5x10^6$ H460 cells by subcutaneous injection. Treatment was started after the tumor volumes reached ~100-150 mm^3 in volume. The mice were randomly assigned into treatment groups (n=5), and IEP-PEG or free EP were injected. Injections were performed every other day for a total of 4 injections at an EP dose of 5 mg/kg. Tumor sizes were measured every other day with calipers across their two perpendicular diameters, and the tumor volume was calculated using the following formula: V=0.5 x (WxWxL), where V is tumor volume, W is the smaller perpendicular diameter and L is the larger perpendicular diameter. Body weight of each mouse was recorded every other day to assess any toxicity.

TUNEL and Immunohistochemistry Assay:

In vivo tumor cell apoptosis was determined by TdT-mediated dUTP Nick-End Labeling (TUNEL) assay. H460 tumor bearing mice were given three daily IV injections of IEP-PEG or free EP at a dose of 5 mg/kg (n=3). Twenty-four hours after the final injection, mice were sacrificed and tumors were fixed in 4% paraformaldehyde solution for 12 h before being embedded in paraffin and sectioned at a thickness of 5 μm. The TUNEL staining was performed as recommended by the manufacturer (Promega). DAPI mounting medium (Vector Laboratories, Inc., Burlingame, CA) was dropped on the sections for nuclear staining. Images of TUNEL-

stained tumor sections were obtained by using a fluorescence microscope (Nikon Corp., Tokyo, Japan). The percentage of apoptotic cells was obtained by dividing the number of apoptotic cells (TUNEL positive cells shown as green dots) by the number of total cells (blue nuclei stained by DAPI, not shown) in each microscopic field, and 10 representative fields were randomly selected in each treatment group for this analysis. Proliferation of tumor cells after the aforementioned treatments and dosing schedule was detected by immunohistochemistry, using an antibody against proliferating cell nuclear antigen (PCNA) (1:200 dilution, Santa Cruz). The immunohistochemistry was performed using a mouse-specific HRP/DAB detection IHC kit as recommended by the manufacturer (Abcam, Cambridge, MA). The percentage of proliferating cells was obtained by dividing the number of PCNA positive cells (shown as brown dots) by the number of total cells (blue nuclei stained by hematoxylin) in each microscopic field, and 10 representative microscopic fields were randomly selected in each treatment group (n=3) for quantification.

***In vivo* safety studies:**

CD-1 mice were intravenously treated with 5 mg/kg IEP-PEG particles every other day for a total of three injections. One day after the third injection, mice were sacrificed and organs were collected and fixed in 4% paraformaldehyde solution followed by H&E staining. The pictures were taken using a bright field microscope (Nikon, Japan).

Statistical analysis:

Results were expressed as a mean ± standard deviation (SD) and were compared among different groups using Student's t-test. $P < 0.05$ was considered as statistically significant.

Results:

Characterization of IEP-PEG nanoparticles:

Indium and etoposide phosphate were precipitated in a reverse micro emulsion as described above to generate the IEP nanoparticle cores, which were analyzed using high resolution TEM to evaluate their morphology and size. Stable cores could be fabricated as small nanoparticles with a diameter of only ~5 nm. Energy dispersive X-ray spectroscopy (EDS) confirmed the presence of indium and phosphate in the cores (Fig. 1A). The amount of etoposide phosphate (EP) encapsulated in the DOPA-stabilized IEP core was measured by UV-Vis spectroscopy (Fig. 1B) by using a standard curve for free EP. Using this method, we found that 60-65% of the drug was encapsulated in the nanoparticles. The structure of EP from lysed IEP nanoparticles was analyzed by ESI-MS (Fig. 1C) and showed that free and nanoparticle-associated EP had similar mass, confirming that the structure of the drug was not changed by the nanoparticle preparation process (data not shown). Final particles were generated by coating the cores with DOPC, cholesterol, and DSPE-PEG2000 to form an outer leaflet for the lipid bilayer, lengthen time in circulation, and enhance tumor accumulation. After lipid film hydration, TEM images show that the small particle cores aggregate to form slightly larger particle conglomerates with an average size of ~55nm as calculated by TEM (Fig. 1D) and dynamic light scattering (DLS) (Fig. 1E). Using DLS, the zeta potential was -40 mV for the final IEP-PEG particles (Fig. 1F).

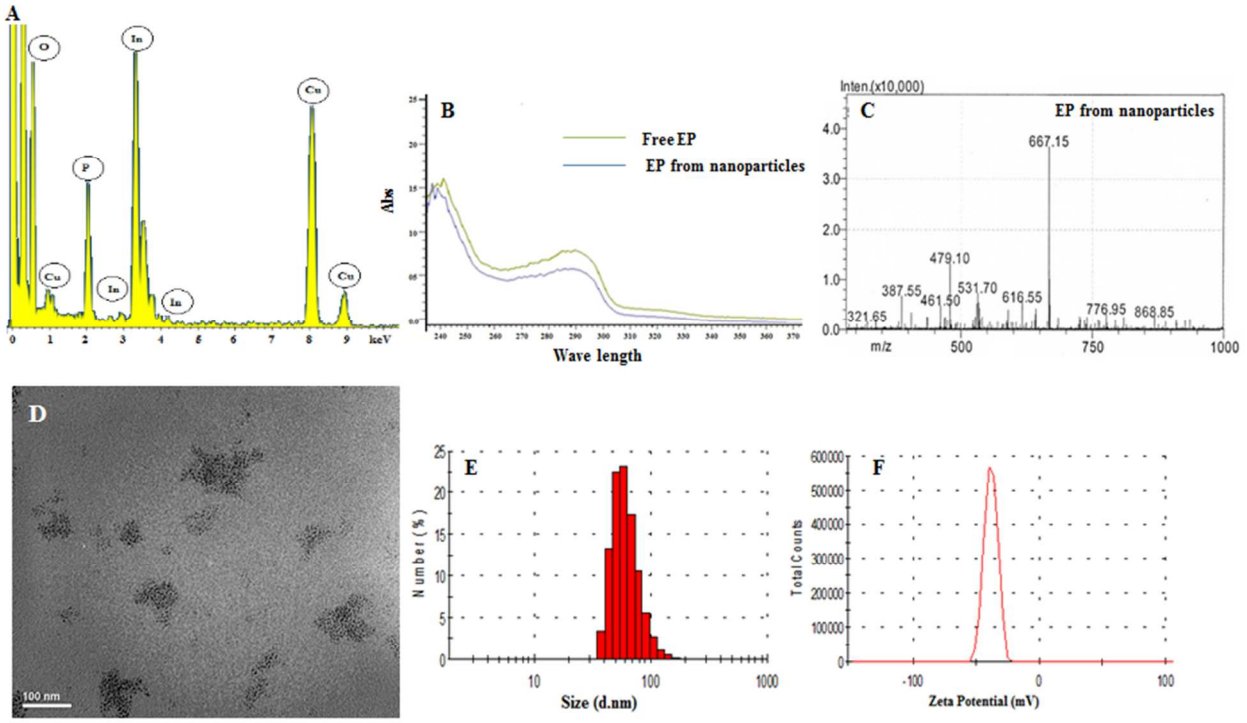

Fig. 1: Characterizations of IEP nanoparticles; A) EDS spectrum of IEP-PEG nanoparticles; B) UV/Vis absorption spectrum comparing free EP and EP dissociated from IEP-PEG nanoparticles; C) ESI-MS for EP encapsulated in nanoparticles. D) TEM image of final IEP-PEG nanoparticles; E) hydrodynamic size of IEP-PEG nanoparticles using DLS; F) Zeta potential of IEP-PEG nanoparticles using DLS.

***In vitro* cellular uptake of IEP-PEG:**

The unorthodox final particle structure necessitated confirmation that these particles could indeed enter into tumor cells. IEP-PEG was dual-labeled with NBD-DOPA (green) to show successful inner leaflet lipid coating during core formation, and also with the small molecule DiI (red) to show the presence of a lipid bilayer in the final particle. IEP-PEG was incubated with H460 cells *in vitro* for 4 h before washing and fixing the cells for analysis. Fig. 2 shows that

both DiI and NBD accumulate in cells, suggesting that the IEP-PEG particles are able to enter the cells intact.

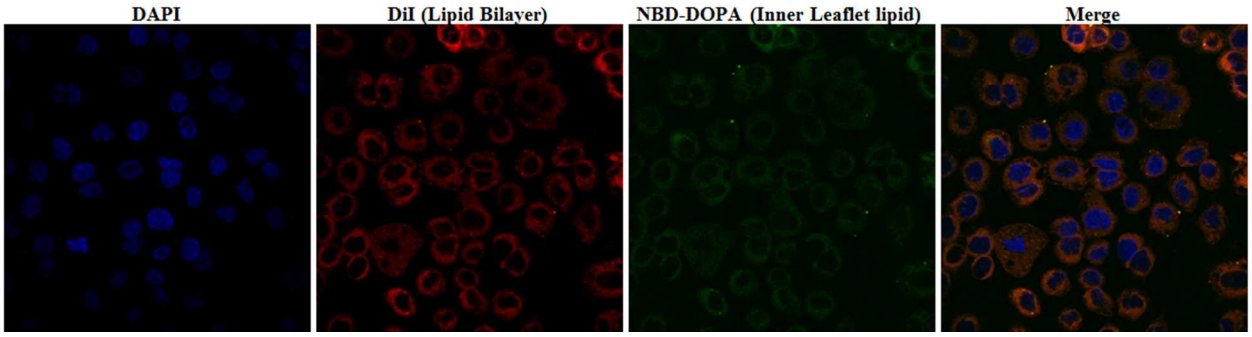

Fig. 2: Cellular uptake of dual-labeled IEP-PEG nanoparticles in H460 cells *in vitro*. Cell nucleus labeled with DAPI; inner leaflet lipids labeled with NBD-DOPA; lipid bilayer labeled with DiI.

***In vitro* release and anti-cancer activity of IEP-PEG nanoparticles:**

The release profile of IEP-PEG was measured to determine the stability of the particles in PBS at a pH of 7.4 and 5.0. The release profile showed a slow, steady release of drug with no burst release (Figure 3A). This release was not acid sensitive, which was not surprising, given the low Ksp of phosphate and indium.

The *in vitro* anti-cancer activity of IEP-PEG nanoparticles was measured by an MTT assay in a cultured NCI- H460 lung carcinoma cell line that was incubated with a range of formulations for four h before changing the media and incubating for another 36 h. The cells experienced a dose-dependent toxicity from IEP-PEG nanoparticles and free EP, but free $InCl_3$ and free outer leaflet liposomes did not cause any toxicity (Fig. 3A).

Mechanisms of cell death from 25 μM EP *in vitro* were also determined. Cells were incubated with IEP-PEG and controls for 24 h before collection and measurement. The DNA

damage caused by EP induces apoptosis through the activity of caspase-type proteases,[23] primarily caspases 3 and 7. Compared to the untreated control, the amount of these apoptotic caspases in cultured H460 cells was 6-fold higher when treated with IEP-PEG nanoparticles and 5-fold higher when treated with free EP (Fig. 3B). Indium chloride alone had no effect on caspase 3/7 upregulation. Poly ADP ribose polymerase (PARP-1) expression was also measured to determine apoptotic mechanisms of EP. PARP-1, a 113 kDa enzyme involved in DNA repair, is known to be cleaved by caspases into 24 kDa and 89 kDa fragments during the execution of apoptosis.[24] The 89 kDa cleavage product was readily detectable in cells treated with IEP-PEG nanoparticles or free etoposide phosphate (Fig. 3C), while free indium chloride again presented no toxic effect.

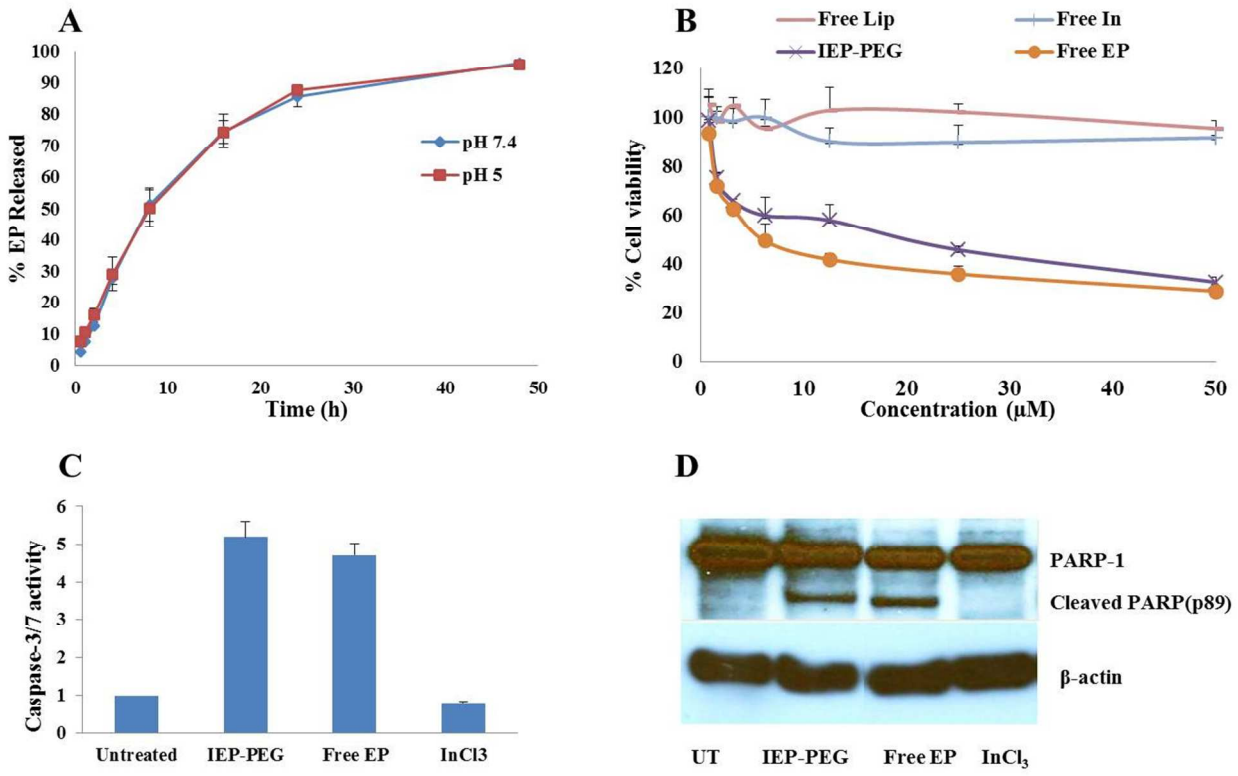

Fig. 3: *In vitro* release, cytotoxicity, and mechanistic studies of IEP-PEG nanoparticles in H460 treated cells; A) etoposide phosphate release from IEP in 37°C PBS at pH 7.4 or pH 5; B) MTT assay; C) Caspase activation; D) Western blot for PARP-1 cleavage; data in A-C presented as mean ± SD, n=3.

Effect of EP on cell cycle progression:

We further evaluated the effect of IEP-PEG nanoparticles on the cell cycle using flow cytometry. Etoposide inhibits topoisomerase II, resulting in DNA strand breakage which in turn causes cell cycle arrest at late S or early G2/M phase.[25] Analysis of cell cycle progression using flow cytometry (Fig. 4) demonstrated that 59% of the cells treated with IEP-PEG nanoparticles and 47% of cells treated with free EP were arrested at G2/M phase. Cells treated with free $InCl_3$ had no discernable effect on cell cycle progression compared to the control.

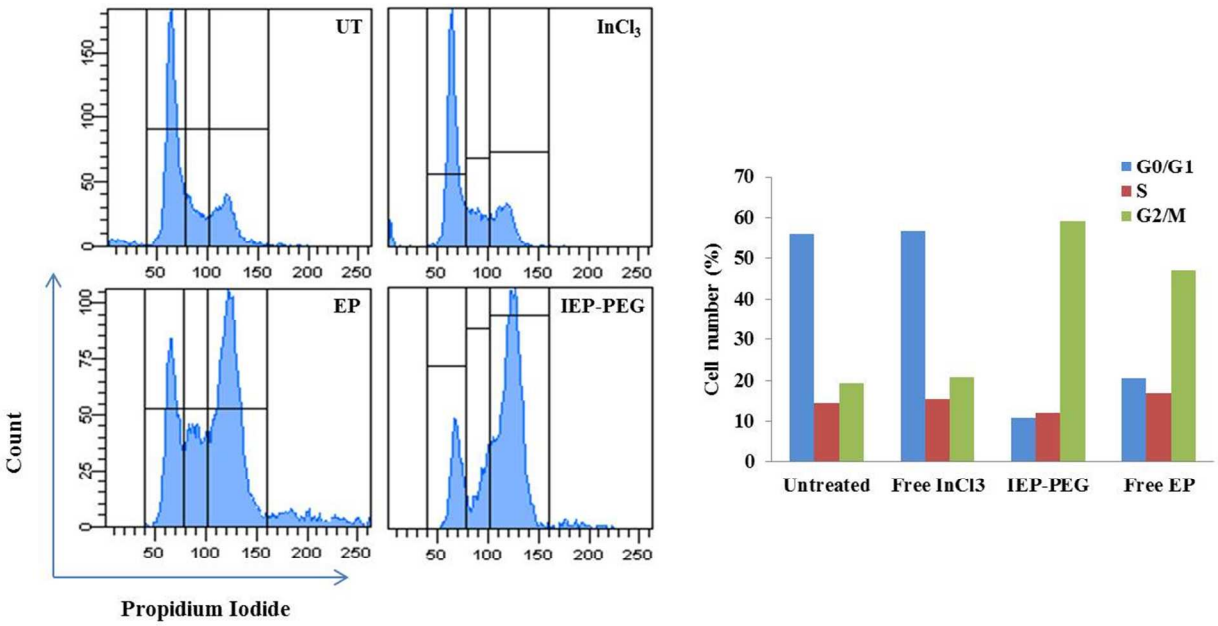

Fig. 4: Analysis of cell cycle arrest via flow cytometry 24 h after treatment with 25 μM EP. EP and IEP-PEG both showed inhibition of cell cycle progression at G2/M phase.

***In vivo* Bio-distribution of IEP-PEG nanoparticles:**

After successful *in vitro* delivery and treatment using IEP-PEG, we analyzed pharmacokinetics and bio-distribution of the nanoparticles using the radioisotope. ^{111}In, a radioisotope of indium, emits high energy gamma rays that are detectible via gamma scintillation and SPECT imaging. ^{111}In was incorporated into IEP by mixing a trace amount of ^{111}In with the EP aqueous phase just before particle fabrication. The low concentration of ^{111}In could then begin to associate with the bulk EP before nonradioactive indium could competitively inhibit ^{111}In encapsulation. Using this method, ^{111}In incorporation into IEP was ~50%.

Pharmacokinetic analysis of ^{111}IEP-PEG shows that the particles cleared quickly from circulation after i.v. injection. As shown in Fig. 5A and Fig. 5B that the bio-distribution of these particles does not change greatly between 2h and 24h after injection. These results were also supported by SPECT imaging, which was also used by this theranostic particle to show ^{111}IEP-PEG bio-distribution and tumor accumulation (Fig. 5C). While the dose of ^{111}In was higher for the SPECT study than for the other bio-distribution studies, the dose of EP and of IEP particles remained constant. This was achieved by adding different amounts of trace ^{111}In to the particles during fabrication, which can vary the radioloading density while maintaining the particle batch size.[26]

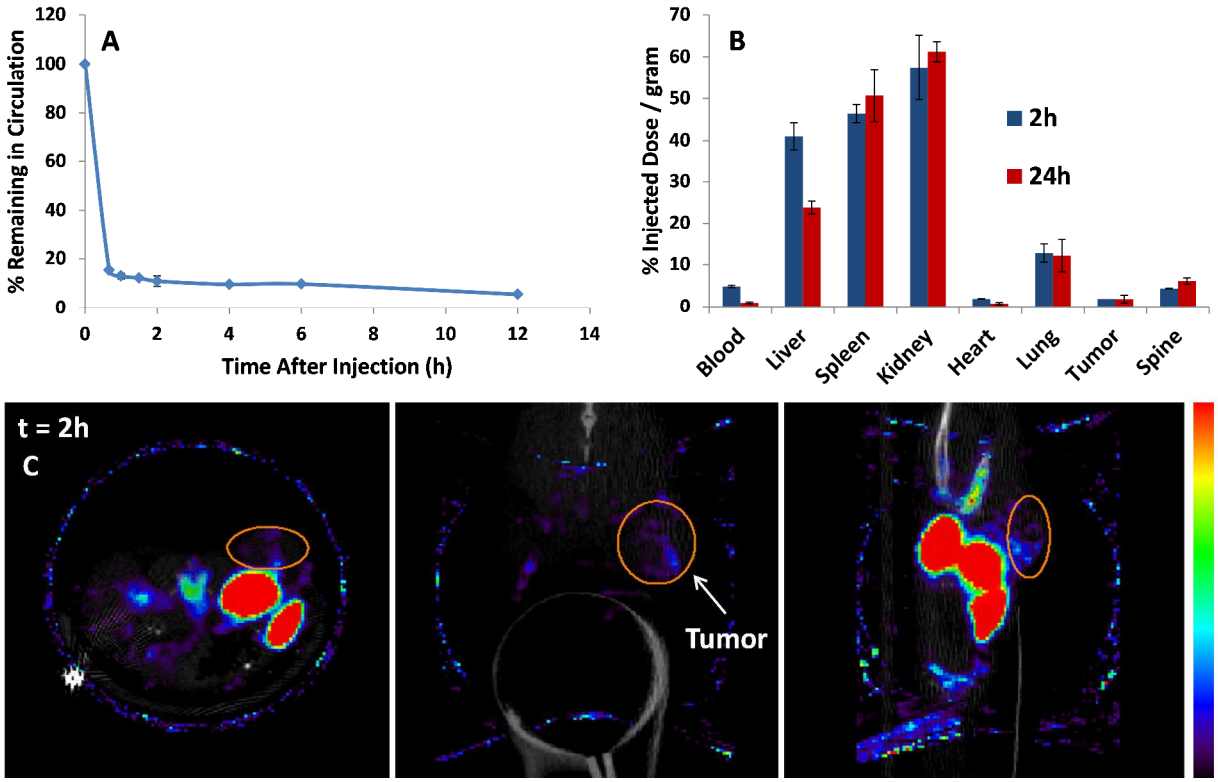

Fig. 5: Biodistribution of IEP-PEG: A) Pharmacokinetics of ^{111}IEP-PEG; B) Organ biodistribution of ^{111}IEP-PEG 2h (n=2) and 24h (n=3) after treatment; C) SPECT/CT images of ^{111}IEP-PEG 2h after injection, from left to right: axial, coronal, and saggital views.

***In vivo* tumor growth inhibition:**

We next evaluated the antitumor efficacy of IEP-PEG nanoparticle formulations in a mouse H460 xenograft tumor model. Tumor-bearing nude mice were intravenously injected with nanoparticles or free EP every other day for a total of four injections. Treatment with IEP-PEG nanoparticles significantly inhibited tumor growth relative to free EP (Fig. 6). This may be due to IEP-PEG's ability to take advantage of the tumor's enhanced permeability and retention, while free EP is easily degradable at physiological pH and may also be cleared quickly by the

kidneys.[27] The body weight of the treated mice did not change significantly over the course of the study, suggesting that there was no systemic toxicity as a result of the treatment.

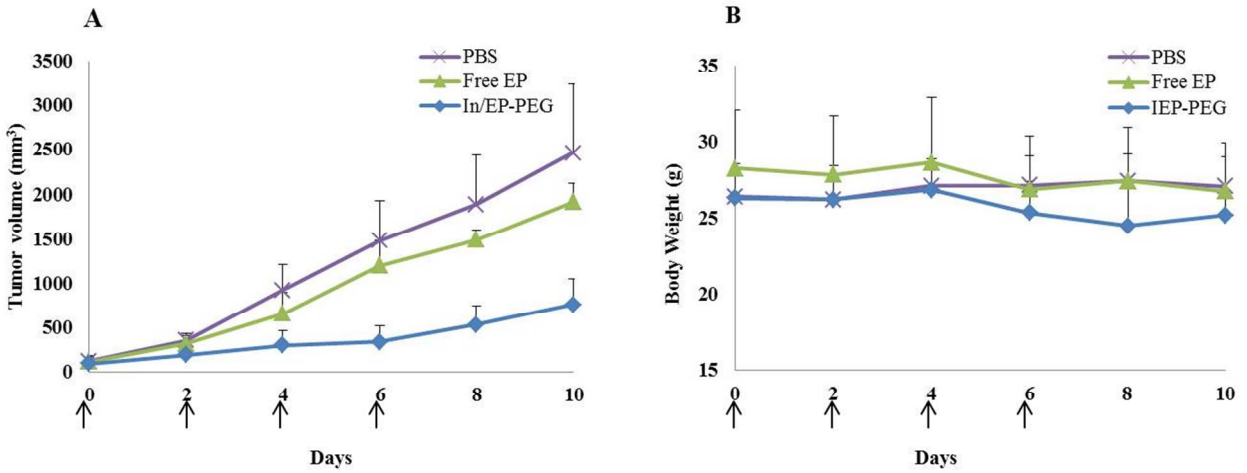

Fig. 6: *In vivo* therapeutic effect of IEP-PEG nanoparticles in a H460 xenograft mouse tumor model; A) tumor growth inhibition; B) Body weight change, data represent mean ± SD, n=5; *p< 0.005; PBS *vs.* In/EP-PEG); arrows indicate the injection schedule.

IEP-PEG-induced tumor cell proliferation inhibition and apoptosis *in vivo*:

After showing successful tumor growth inhibition, tumor cell apoptosis from this *in vivo* treatment was evaluated by the TUNEL assay. The assay is commonly used to detect fragmented DNA in apoptotic cells by using fluorescently labeled dUTP. Upon detection, apoptotic cells appear as dots of green fluorescence in tumor sections (Fig. 7, upper panels). The percentage of tumor cells that were apoptotic was significantly higher after treatment with nanoparticles, but not free drug (Fig. 7A).

Proliferating cell nuclear antigen (PCNA) expression, known to be increased in actively proliferating cells, was used to evaluate the extent of cell proliferation in xenograft tumors after treatment (Fig. 7, lower panels). PCNA was detected by immunohistochemistry in Fig. 7B, and while tumor sections from untreated mice or mice given free EP contained 75-80% proliferative cells, tumor sections from mice treated with IEP-PEG contained only 10-20% proliferative cells. Our nanoparticle system appears to effectively induce apoptosis and inhibit cell proliferation within tumors by increasing the bioavailability of systemically administered EP.

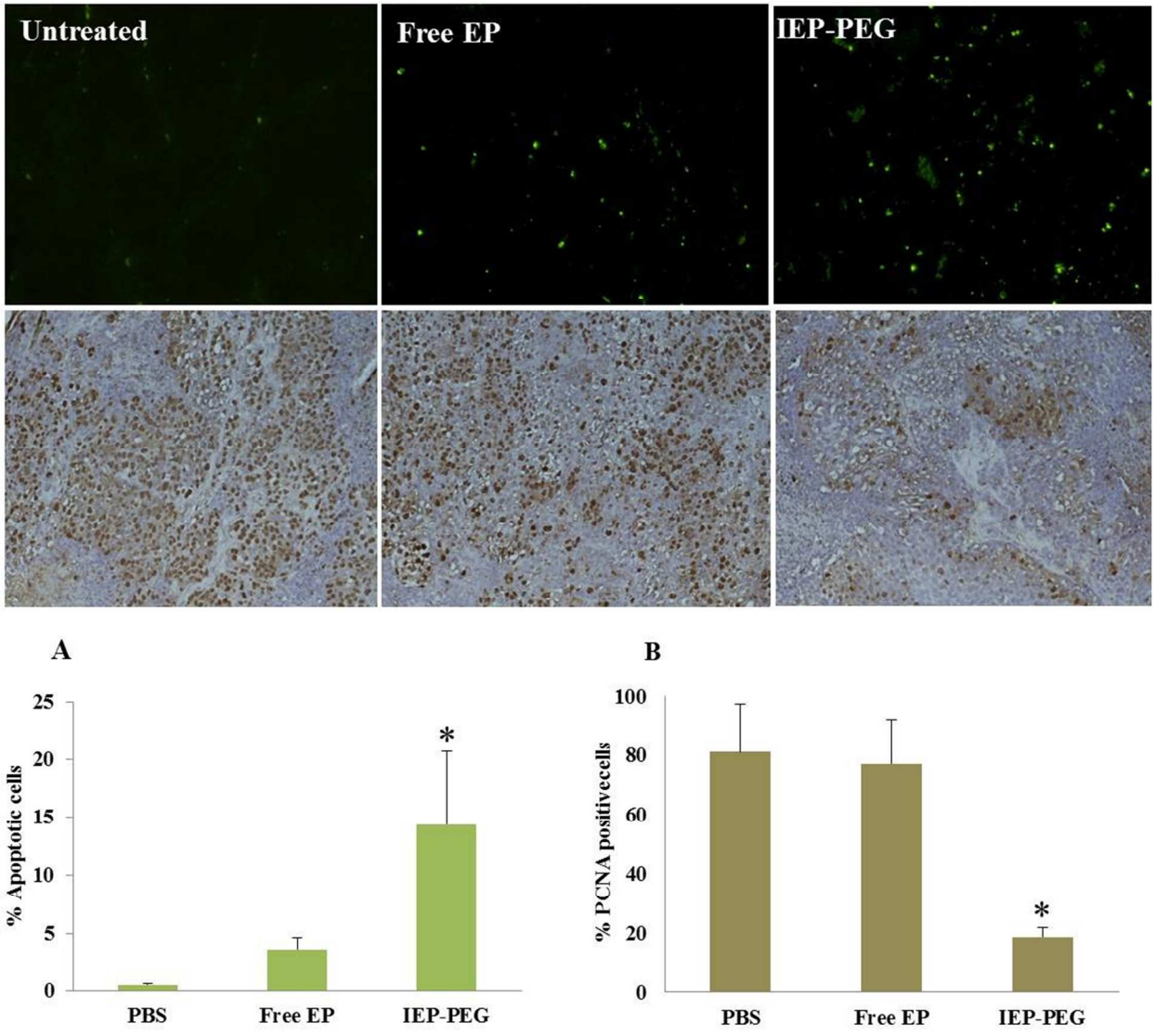

Fig. 7: IEP-PEG nanoparticles triggered tumor cell apoptosis and inhibited cell proliferation: Tunnel assay (upper panels) and PCNA analysis (lower); A) Tunnel assay quantification *p<0.006 for Free EP *vs.* In/EP-PEG; B) PCNA *p<0.0001 for Free EP vs. In/EP-PEG, n=3.

***In vivo* safety study:**

To further test the safety profile of free EP and IEP-PEG, we analyzed the systemic toxicity of nanoparticles via histopathology analysis of organs taken from mice treated with EP or IEP-PEG nanoparticles (Fig. 8). At those given schedule, there were no indicators of significant toxicity observed in organs from mice treated with EP or IEP-PEG when compared to those from untreated mice.

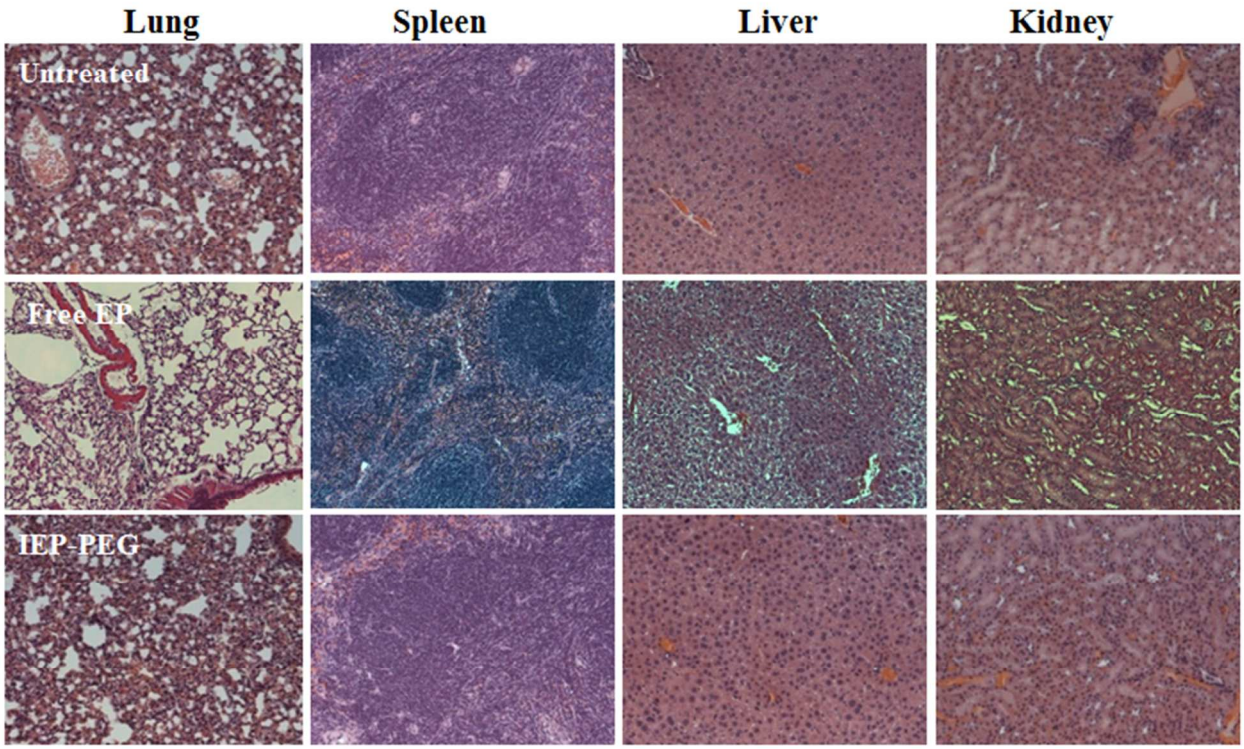

Fig. 8: H&E analysis of mouse major organs treated with EP or IEP-PEG nanoparticles shows no morphological toxicity associated with the treatment (n=3).

Discussion:

In the present study, we developed a new, indium-based, theranostic nanoparticle system for cancer therapy and imaging. Effective administration of the widely used anticancer drug, etoposide, is complicated by limitations stemming from its hydrophobicity, lack of solubility, and toxicity. The water-soluble analog, EP, offers some improvement but bioavailability and toxicity still remain a problem. Here we used indium both as a carrier for EP and as an imaging agent (^{111}In) to allow nanoparticle synthesis of EP in addition to enabling SPECT imaging via ^{111}IEP-PEG. Lipid-coated IEP-PEG nanoparticles were synthesized using a reverse micro emulsion method and then characterized in terms of shape and size. Although etoposide and etoposide phosphate are susceptible to degradation through epimerization of the lactone ring [28], our formulation did not alter the EP structure, as confirmed by UV and ESI-MS (Fig. 1). Because surface functionality determines the fate of circulating nanoparticles *in vivo*, we modified the nanoparticle surface with PEG, a widely-used hydrophilic polymer, to increase particle dispersion during fabrication, allow some escape from macrophage phagocyte system (MPS) uptake[9] and prolong time in circulation. Cytotoxicity studies in NCI-H460 lung cancer cell lines suggest that these nanoparticles efficiently deliver EP to tumor cells and exhibit dose-dependent anti-tumor activity at a level similar to the free drug. We believe that after endocytosis, EP is dissociated from indium in the sink condition, and the released EP is converted to etoposide by intracellular phosphatases to achieve its cytotoxic effects.[29] Because no significant cytotoxicity was observed from treatment with free $InCl_3$, we suspect that this low dose of indium dose may be safe for use.

Anti-cancer effects were also evaluated in an H460 xenograft tumor-bearing mouse model, where IEP-PEG nanoparticles exhibited anti-tumor activity in mice (Fig. 6). While free EP showed efficacy similar to IEP-PEG *in vitro*, the *in vivo* data presented here show that IEP-PEG outperforms free EP in tumor growth inhibition, apoptotic cell generation, and inhibition of cell proliferation without inducing toxicity to normal tissue. The added value of IEP-PEG *in vivo* may be caused by the greater bioavailability of IEP-PEG allowed by the tumor's enhanced permeability and retention of nanoparticles in the tumor environment relative to small molecules, as bio-distribution and drug release studies show that the IEP nanoparticles remain in the tumor after 24h and release the drug slowly. Future work with this system will include studies focused on improving pharmacokinetics and specific accumulation into tumor cells, such as modifying the composition of the outer leaflet lipids and conjugating targeting ligands to the particles.

Conclusions:

In conclusion, we have successfully encapsulated the anti-cancer prodrug etoposide phosphate using an indium-based theranostic nanoparticle system. *In vitro* cytotoxicity studies and *in vivo* antitumor experiments reveal the efficacy of this nanoparticle formulation for delivery of the anticancer drug EP. ^{111}IEP-PEG was also used as a theranostic agent for SPECT imaging, allowing simultaneous delivery of both an imaging agent and an anti-cancer drug with a single nanoparticle system.

Acknowledgements:

The authors graciously thank NIH funding sources (grants CA151652, CA149363). ABS was supported by the National Science Foundation Graduate Research Fellowship. We thank

Amar Kumbhar and Wallace Ambrose, with the Institute for Advanced Materials, NanoScience and Technology at UNC, for help with the TEM. Dr Keduo Qian, division of medicinal chemistry, UNC is thanked for the use of their mass spectroscopy instrument. We thank Steven Plonk for assistance in editing the manuscript, and we thank Dr. Feng Liu for thoughtful discussions.

References:

1. K. R. Hande, *Eur J Cancer*, 1998, **34**, 1514-1521.
2. A. K. Larsen, A. Skladanowski and K. Bojanowski, *Progress in cell cycle research*, 1996, **2**, 229-239.
3. S. Z. Fields, L. N. Igwemezie, S. Kaul, L. P. Schacter, R. J. Schilder, P. P. Litam, B. S. Himpler, C. McAleer, J. Wright, R. H. Barbhaiya and et al., *Clinical cancer research : an official journal of the American Association for Cancer Research*, 1995, **1**, 105-111.
4. W. C. Rose, G. A. Basler, P. A. Trail, M. Saulnier, A. R. Crosswell and A. M. Casazza, *Investigational new drugs*, 1990, **8 Suppl 1**, S25-32.
5. P. D. Senter, M. G. Saulnier, G. J. Schreiber, D. L. Hirschberg, J. P. Brown, I. Hellstrom and K. E. Hellstrom, *Proceedings of the National Academy of Sciences of the United States of America*, 1988, **85**, 4842-4846.
6. J. R. Heath and M. E. Davis, *Annual review of medicine*, 2008, **59**, 251-265.
7. *Nature reviews. Drug discovery*, 2007, **6**, 174-175.
8. J. Fang, H. Nakamura and H. Maeda, *Advanced drug delivery reviews*, 2011, **63**, 136-151.
9. S. Ramishetti and L. Huang, *Therapeutic delivery*, 2012, **3**, 1429-1445.
10. C. Chen, X. X. Xie, Q. Zhou, F. Y. Zhang, Q. L. Wang, Y. Q. Liu, Y. Zou, Q. Tao, X. M. Ji and S. Q. Yu, *Nanotechnology*, 2012, **23**, 045104.
11. W. Y. Qian, D. M. Sun, R. R. Zhu, X. L. Du, H. Liu and S. L. Wang, *International journal of nanomedicine*, 2012, **7**, 5781-5792.
12. A. Lamprecht and J. P. Benoit, *Journal of controlled release : official journal of the Controlled Release Society*, 2006, **112**, 208-213.
13. R. S. Kalhapure and K. G. Akamanchi, *Colloids and surfaces. B, Biointerfaces*, 2013, **105**, 215-222.
14. M. Callewaert, S. Dukic, L. Van Gulick, M. Vittier, V. Gafa, M. C. Andry, M. Molinari and V. G. Roullin, *Journal of biomedical materials research. Part A*, 2013, **101**, 1319-1327.
15. M. Snehalatha, K. Venugopal, R. N. Saha, A. K. Babbar and R. K. Sharma, *Drug delivery*, 2008, **15**, 277-287.
16. S. Shah, A. Pal, R. Gude and S. Devi, *J Appl Polym Sci*, 2013, **127**, 4991-4999.
17. B. C. Tang, J. Fu, D. N. Watkins and J. Hanes, *Biomaterials*, 2010, **31**, 339-344.
18. D. Psimadas, P. Georgoulias, V. Valotassiou and G. Loudos, *Journal of pharmaceutical sciences*, 2012, **101**, 2271-2280.
19. S. S. Kelkar and T. M. Reineke, *Bioconjugate chemistry*, 2011, **22**, 1879-1903.
20. K. J. Kairemo, H. A. Ramsay, M. Tagesson, A. P. Jekunen, T. K. Paavonen, H. A. Jaaskela-Saari, K. Liewendahl, K. Ljunggren, S. Savolainen and S. E. Strand, *European journal of nuclear medicine*, 1996, **23**, 631-638.

21. K. J. Kairemo, H. Ramsay, T. K. Nikula, E. V. Hopsu, M. J. Taavitsainen, S. Bondestam and J. V. Hiltunen, *J Nucl Biol Med*, 1994, **38**, 135-139.
22. Y. Zhang, W. Y. Kim and L. Huang, *Biomaterials*, 2013, **34**, 3447-3458.
23. R. J. Sleiman and B. W. Stewart, *Clinical cancer research : an official journal of the American Association for Cancer Research*, 2000, **6**, 3756-3765.
24. G. V. Chaitanya, A. J. Steven and P. P. Babu, *Cell communication and signaling : CCS*, 2010, **8**, 31.
25. P. J. Smith, S. Soues, T. Gottlieb, S. J. Falk, J. V. Watson, R. J. Osborne and N. M. Bleehen, *British journal of cancer*, 1994, **70**, 914-921.
26. A. B. Satterlee, H. Yuan and L. Huang, *Journal of controlled release : official journal of the Controlled Release Society*, 2015, DOI: 10.1016/j.jconrel.2015.08.048.
27. A. H. Witterland, C. H. Koks and J. H. Beijnen, *Pharmacy world & science : PWS*, 1996, **18**, 163-170.
28. J. H. Beijnen, J. J. M. Holthuis, H. G. Kerkdijk, O. A. G. J. Vanderhouwen, A. C. A. Paalman, A. Bult and W. J. M. Underberg, *Int J Pharm*, 1988, **41**, 169-178.
29. D. M. Karl and D. B. Craven, *Applied and environmental microbiology*, 1980, **40**, 549-561.